Kim *et al. Robomech J* (2019) 6:3
https://doi.org/10.1186/s40648-019-0131-4

ROBOMECH Journal

RESEARCH ARTICLE Open Access

# Caging-based grasping of deformable objects for geometry-based robotic manipulation

Dabae Kim[1], Yusuke Maeda[2*] and Shun Komiyama[3]

**Abstract**

In this paper, we present a novel method for caging-based grasping of deformable objects. This method enables manipulators to grasp objects simply with geometric constraints by using position control of robotic hands, and not through force controls or mechanical analysis. Therefore, this method has cost benefits and algorithmic simplicity. In our previous studies, we mainly focused on caging-based grasping of rigid objects such as 2D/3D primitive-shaped objects. However, considering realistic objects, manipulation of deformable objects is also required frequently. Hence, this study is motivated to manipulate deformable objects, adopting a caging-based grasping approach. We formulate caging-based grasping of deformable objects, and target three types of deformable objects: a rigid object covered with a soft part, a closed-loop structure, and two rigid bodies connected with a string, which can be regarded as primitive shapes. We then derive concrete conditions for grasp synthesis and conduct experimental verification of our proposed method with an industrial manipulator.

**Keywords:** Robotic manipulation, Caging, Grasping, Caging-based grasping, Deformable objects

## Background

For manipulating objects via robotic hands, object restraint methods are usually adopted. These methods aim to eliminate the movement of objects by constraining objects. One of the object restraint methods, the grasping approach [1, 2], which restrains objects by using force controls, is commonly adopted as shown in Fig. 1a (we call this approach "Grasping", simply). Grasping has an advantage in that it is possible to uniquely determine the pose (position/orientation) of objects, so that accurate manipulation can be realized. However, it requires mechanical analysis or force sensing using expensive equipment. These requirements lead to a high cost and algorithmic complexity, even if objects do not need to be manipulated in extremely precise conditions.

On the other hand, the caging approach [3, 4] is also introduced as an object restraint method, which cages objects using position controls as shown in Fig. 1b (we call this approach "Caging", simply). In general, rigid objects are caged by multiple agents in [5, 6], whereas [7, 8] are recently conducted by robotic hands. When caging is realized, rigid objects cannot escape from the robotic hands physically, even if the objects take any possible pose. Caging enables robotic hands to restrain objects without using mechanical analysis or force sensing, in contrast to grasping. However, it cannot determine object poses uniquely, so it has to be performed when manipulating objects roughly. In other words, although caging is not a more accurate approach than grasping, it is an effective approach from the viewpoint of enhancing the versatility of manipulation with a simple algorithm. Comparing grasping and caging, it can be said that there are advantages and disadvantages, and it is necessary to choose the proper approach in accordance with manipulating situations.

This study is motivated by the possibility to adopt the advantages of both the grasping and caging approaches, which constrain objects by using only simple position control. We call this approach caging-based grasping [9],

*Correspondence: maeda@ynu.ac.jp
[2] Faculty of Engineering, Yokohama National University, 79-5 Tokiwadai, Hodogaya-ku, 240-8501 Yokohama, Japan
Full list of author information is available at the end of the article

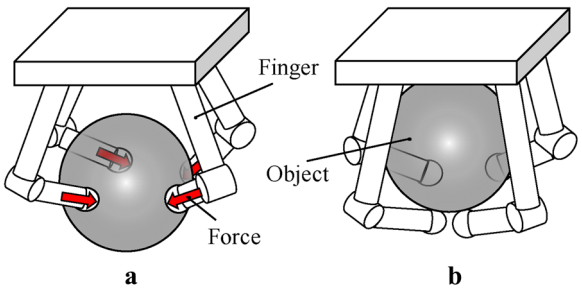


**Fig. 1** Object restraint methods. **a** Grasping and **b** caging approaches

as shown in Fig. 2. Caging-based grasping is defined by two main conditions: rigid-part caging condition and soft-part deformation condition. The rigid-part caging condition denotes a complete imprisonment of the rigid parts of objects by the rigid parts of robotic hands. However, there is a free space in which the object can move, though the object is caged. Hence, in caging-based grasping, we set the soft-part deformation condition, which disallows objects to move via the deformation of the soft part.

In our previous studies [9, 10], we formulated caging-based grasping, derived concrete conditions with geometric constraints, and confirmed that 2D/3D caging-based grasping can be realized by experimental verification. However, the studies were restricted to rigid objects, which cannot be deformed by external force. Most caging studies also consider rigid objects or their equivalents only (e.g., [11–14]). However, caging deformable objects is conducted in [15, 16]. Gopalakrishnan and Goldberg [15] defines "D-space" by modeling deformable objects as linear and elastic polygons, and [16] computes topological features such as necks or double forks. For grasping deformable objects, [17, 18] worked with deformable viscid objects with FEM analysis based on linear/non-linear theory considering a friction cone. As another grasping approach, vision-based grasping of deformable objects in real time is also conducted in [19–21], which requires mechanical analysis or FEM analysis. However, the above studies require difficult modeling for deformable objects. In this paper, we focus on caging-based grasping of deformable objects with simple geometry-based algorithms, and aim to extend the versatility of caging-based grasping.

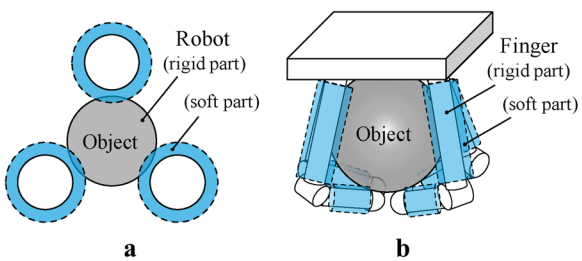


**Fig. 2** Caging-based grasping approach. **a** 2D and **b** 3D

## Problem statement

As models of deformable objects, we set three types: a rigid object covered with a soft part, a closed-loop structure, and two rigid bodies connected with a string as shown in Fig. 3. The reason we set these types is that they can be regarded as primitive shapes of deformable objects such as stuffed toys, chains, and wire harnesses, respectively. From now, for each of the object types, we present applicable robot hands and concrete methods for caging-based grasping.

The rigid object covered with a soft part is a rigid body, which has a soft part around it. In this paper, we consider 2D primitive shapes including crosses, circles, and rectangles. The soft part indicates elastic bodies, which generate reaction forces when deformed by external forces. Rigid-fingered hands are used as robotic hands for 2D caging-based grasping, which is conducted via deformations of the soft parts of objects.

The closed-loop structure has one closed loop, composed of rigid links and rotation joints. Rigid-fingered hands with soft parts are used as robotic hands for 2D caging-based grasping, which is conducted via deformations of the soft parts of robotic hands.

The two rigid bodies connected with a string consist of two 3D rigid bodies such as spheres, cuboids, and cylinders that are connected with a string. Parallel grippers with soft parts are used as robotic hands for 3D caging-based grasping, which is made possible because of the deformations of the soft parts of robotic hands.

Caging-based grasping conditions of deformable objects are formed by only geometric constraints, whereas there are also mechanical constraints which are complicate to deal with and require high computational cost. For these reasons, we assume: (1) the position control of the hand is perfect even if a reaction force is given by the object, and (2) the reaction force by the deformation of the object/hand soft part is not large enough to destroy the object or hand.

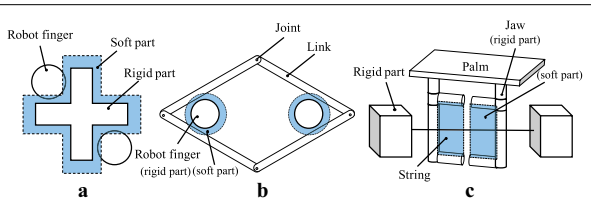


**Fig. 3** Three types of deformable objects. **a** Rigid object covered with a soft part, **b** closed-loop structure, and **c** two rigid bodies connected with a string

## Caging-based grasping

In this section, we define and formulate the caging-based grasping of deformable objects, based on our previous study [9]. Note that [9] handles the object of the caging-based grasping as rigid bodies, whereas this paper extends to deformable objects. Hence, we change the definition and formulation partially, considering the following:

- Objects are deformable.
- Soft parts may be located on objects as well as hands.

### Definition

The caging-based grasping condition of deformable objects consists of the "Rigid-part caging condition" and the "Soft-part deformation condition", which consider the movements and deformable ranges of the objects:

- Rigid-part caging condition: The object is caged in a closed region formed by the rigid parts of a robot hand. This condition consists of the following three sub-conditions:
  (a) Closed region formation: A closed region through which the object cannot pass is formed by the rigid parts of the robot hand.
  (b) Object inside: The object is within the closed region formed by the rigid parts of the robot hand.
  (c) No interference: The rigid parts of the robot hand do not overlap with the rigid parts of the object.
- Soft-part deformation condition: Assuming that the soft parts of the robot hand and/or the object become rigid, the closed region for caging in the configuration space of the object becomes empty.

The caging-based grasping condition can be established without explicit mechanical analysis or force sensing by satisfying the two conditions above.

### Formulation

Here we explain the formulation of caging-based grasping. Symbols are defined as mentioned below (Fig. 4):

- $n$: Number of rigid robot bodies.
- $C$: Configuration space of the rigid parts of the object for their movements.
- $\mathcal{A}_{\mathrm{obj}}$: Occupied region in real space of rigid parts of the object.
- $\mathcal{A}'_{\mathrm{obj}}$: Occupied region of the entire object including rigid and soft parts in real space without deformations of soft parts.

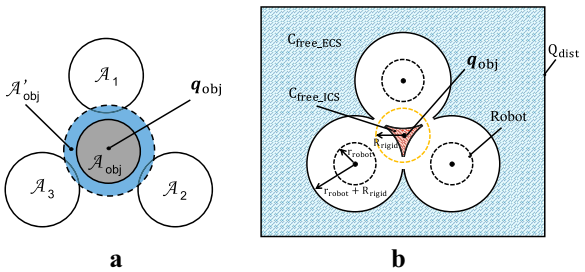


**Fig. 4** Definition of symbols. **a** Real space and **b** configuration space

- $\mathcal{A}_i$: Occupied region in real space of the $i$-th rigid part of the robot, $(i = 1, \ldots, n)$.
- $\mathcal{A}'_i$: Occupied region of the $i$-th rigid part and its attached soft parts in real spaces without deformations of soft parts.
- $\boldsymbol{q}_{\mathrm{obj}}$: Current configuration of the object.

Firstly, we define the free configuration space, in which the rigid parts of the object can move freely without interfering with the rigid part of the robot $\mathcal{A}_1, \ldots, \mathcal{A}_n$ as follows:

$$\mathcal{C}_{\mathrm{free}} := \left\{ \boldsymbol{q}_{\mathrm{obj}} \in \mathcal{C} \middle| \mathcal{A}_{\mathrm{obj}}(\boldsymbol{q}_{\mathrm{obj}}) \cap \left( \bigcup_{i=1}^{n} \mathcal{A}_i \right) = \emptyset \right\}. \tag{1}$$

Similarly, the free configuration space, in the case where the soft parts of the object and robot are regarded as the rigid parts, is defined as follows:

$$\mathcal{C}'_{\mathrm{free}} := \left\{ \boldsymbol{q}_{\mathrm{obj}} \in \mathcal{C} \middle| \mathcal{A}'_{\mathrm{obj}}(\boldsymbol{q}_{\mathrm{obj}}) \cap \left( \bigcup_{i=1}^{n} \mathcal{A}'_i \right) = \emptyset \right\}. \tag{2}$$

$\mathcal{C}_{\mathrm{free}}$ is the free configuration space where the rigid parts of the object and robot do not interfere each other. This space is divided into two spaces: the space where the object is escapable to "far enough" ($\mathcal{C}_{\mathrm{free\_ECS}}$), and the space where the object is inescapable ($\mathcal{C}_{\mathrm{free\_ICS}}$), as follows:

$$\mathcal{C}_{\mathrm{free\_ICS}} := \mathcal{C}_{\mathrm{free}} \backslash \mathcal{C}_{\mathrm{free\_ECS}}, \tag{3}$$

$$\mathcal{C}_{\mathrm{free\_ECS}} := \bigcup_{\boldsymbol{q}_{\mathrm{obj}} \in \mathcal{Q}_{\mathrm{dist}}} \mathcal{C}_{\mathrm{free\_max}}(\boldsymbol{q}_{\mathrm{obj}}). \tag{4}$$

Note that $\mathcal{Q}_{\mathrm{dist}} (\subset \mathcal{C})$ is the set of the object configuration which can be regarded as "far enough", and $\mathcal{C}_{\mathrm{free\_max}}(\boldsymbol{q}_{\mathrm{obj}})$ is the largest connected subset including the object configuration ($\boldsymbol{q}_{\mathrm{obj}}$) in $\mathcal{C}_{\mathrm{free}}$. When only caging is achieved, the object moves freely within $\mathcal{C}_{\mathrm{free\_ICS}}$. However, when $\mathcal{C}_{\mathrm{free\_ICS}}$ is filled with the soft parts of the robot and the object, the object cannot exist without the deformation of the soft parts, and the object is grasped in $\mathcal{C}_{\mathrm{free\_ICS}}$. Here $\mathcal{C}'_{\mathrm{free\_ICS}}$, and $\mathcal{C}'_{\mathrm{free\_ECS}}$ are defined as follows:

$$\mathcal{C}'_{\text{free\_ICS}} := \mathcal{C}'_{\text{free}} \backslash \mathcal{C}'_{\text{free\_ECS}}, \tag{5}$$

$$\mathcal{C}'_{\text{free\_ECS}} := \bigcup_{\boldsymbol{q}_{\text{obj}} \in \mathcal{Q}_{\text{dist}}} \mathcal{C}'_{\text{free\_max}}(\boldsymbol{q}_{\text{obj}}). \tag{6}$$

Note that $\mathcal{C}'_{\text{free\_max}}(\boldsymbol{q}_{\text{obj}})$ is the largest connected subset including the object configuration $\boldsymbol{q}_{\text{obj}}$ in $\mathcal{C}'_{\text{free}}$.

From the above definitions, the caging-based grasping condition of the deformable object are formulated as follows (Fig. 5):

- Rigid-part caging condition
  - Closed region formation: The rigid parts of the robot form a closed region, through which the object cannot pass no matter how the object is moved or deformed:

$$\exists \mathcal{C}_{\text{closed}} \text{ such that } \mathcal{C}_{\text{closed}} \cap \mathcal{C}_{\text{free\_ECS}} = \emptyset. \tag{7}$$

  - Object inside: The rigid parts of the object exist inside the closed region formed by the rigid parts of the robot:

$$\boldsymbol{q}_{\text{obj}} \in \mathcal{C}_{\text{closed}}. \tag{8}$$

  - No interference: The rigid parts of the robots do not interfere with the rigid parts of the object:

$$\boldsymbol{q}_{\text{obj}} \in \mathcal{C}_{\text{free}}. \tag{9}$$

- Soft-part deformation condition: The object cannot exist in closed regions formed by the rigid-part caging condition, when regarding the soft parts of the robot and the object as rigid bodies:

$$\mathcal{C}'_{\text{free\_ICS}} = \emptyset. \tag{10}$$

The caging-based grasping condition is achieved by satisfying Eq. (10) in addition to Eqs. (7)–(9). In this paper, we conduct experiments of caging-based grasping using a real robotic hand, and in such cases testing Eqs. (8) and (9) is trivial. For this reason, object inside and no interference conditions can be omitted in the following sections.

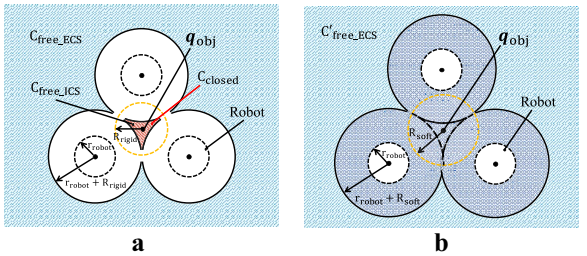


**Fig. 5** Symbols in configuration space. **a** Caging and **b** caging-based grasping

Theoretically perfect caging-based grasping conditions can be derived by strictly following the above formulation. However, exact shapes of the robotic hand and object must be considered, and this is difficult and complicated when deriving the conditions in real problems. To handle these problems, in this paper, we focus on the sufficient conditions of caging-based grasping. This is a tradeoff between obtaining more accurate results and introducing complexity in deriving conditions. In other words, this should be decided according to the requirements of the application.

## Rigid object covered with a soft part

In this section, we introduce a class of the caging-based grasping of the rigid object covered with a soft part. Concretely, we set targets of caging-based grasping as cross-, H-, and U-shaped objects with two-fingered rigid hands, and circular, elliptic, triangular, rectangular, L-shaped, and T-shaped objects with three-fingered rigid hands. In this paper, we representatively introduce concrete conditions of the cross-shaped object with the two-fingered rigid hand for 2D caging-based grasping.

### Hand and object model

As mentioned above, we use the two-fingered rigid hand as the robotic hand. This hand has two circle-shaped 1DOF open/close fingers. The distance between the center of the hand and the fingers ($r_d$) is as shown in Fig. 6a. The cross-shaped object consists of the rigid part and soft part as shown in Fig. 6b. Without loss of generality, we assume that $W_1 - t_1 \leq W_2 - t_2$.

### Rigid-part caging condition

#### *Closed region formation*

Depending on the relationships of parameters between the rigid part of the object and the fingers, the following sufficient conditions are established.

$$\text{(i)}(W_1 - t_1)/2 \geq r, \text{and}\,(W_2 - t_2)/2 \geq r$$

In this case, when the rigid part of the object rotates and two sides of the concave part ($\overline{\text{A}_\text{r}\text{F}}$, $\overline{\text{B}_\text{l}\text{F}}$ or $\overline{\text{C}_\text{r}\text{H}}$, $\overline{\text{D}_\text{l}\text{H}}$) are tangent to one finger whereas one vertex ($\text{D}_\text{l}$ or $\text{A}_\text{r}$) contacts with the other finger, the rigid part of the object is in a critical state as shown in Fig. 7a. The object cannot pass through the space between the two fingers if the distance between the two fingers ($d_{mn}$) is smaller than that of the critical state. Therefore, one sufficient condition is expressed as follows:

$$\begin{cases} d_{mn} - 2r < \min\{W_1, W_2\}, \\ d_{mn} - r < \min\{X_l, X_r\}, \end{cases} \tag{11}$$

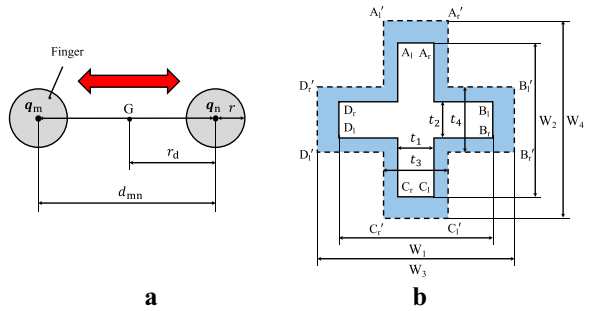


**Fig. 6** Rigid object covered with a soft part. **a** Hand and **b** object model

where

$$\begin{cases} X_l = \sqrt{\{(W_1 + t_1)/2 + r\}^2 + (t_2 + r)^2}, \\ X_r = \sqrt{\{(W_2 + t_2)/2 + r\}^2 + (t_1 + r)^2}. \end{cases}$$

(ii) $(W_1 - t_1)/2 < r$, and $(W_2 - t_2)/2 \geq r$

In this case, when the rigid part of the object rotates and one side of the concave part ($\overline{A_rF}$) is tangent to one finger whereas two vertex ($B_l$ and $D_l$) contacts with the two fingers, the rigid part of the object is in a critical state as shown in Fig. 7b. Therefore, one sufficient condition is expressed as follows:

$$\begin{cases} d_{mn} - 2r < \min\{W_1, W_2\}, \\ d_{mn} - r < Y, \end{cases} \quad (12)$$

where

$$\begin{cases} b = \sqrt{r^2 - \{r - (W_1 - t_1)/2\}^2}, \\ Y = \sqrt{\{(W_1 + t_1)/2 + r\}^2 + (t_2 + b)^2}. \end{cases}$$

(iii) $(W_1 - t_1)/2 < r$, and $(W_2 - t_2)/2 < r$

In this case, two sides of the concave part formed in the object rigid part are tangent to the finger at the vertexes ($A_r$, $B_l$, $D_l$ or $D_l$, $C_r$, $A_r$) which is regarded as the critical state as shown in Fig. 7c. The sufficient condition is expressed as follows:

$$\begin{cases} d_{mn} - 2r < \min\{W_1, W_2\}, \\ d_{mn} - r < \min\{Z_l, Z_r\}, \end{cases} \quad (13)$$

where

$$\begin{cases} Z_l = \sqrt{(W_1 + \sqrt{r^2 - b^2})^2 + (t_2 + b)^2}, \\ Z_r = \sqrt{(W_2 + \sqrt{r^2 - a^2})^2 + (t_1 + a)^2}, \\ a = \frac{1}{2}\left(h + \sqrt{\frac{4k^2r^2}{h^2+k^2} - k^2}\right), \\ b = \frac{1}{2}\left(k + \sqrt{\frac{4h^2r^2}{h^2+k^2} - h^2}\right), \\ k = (W_2 - t_2)/2, \\ h = (W_1 - t_1)/2. \end{cases}$$

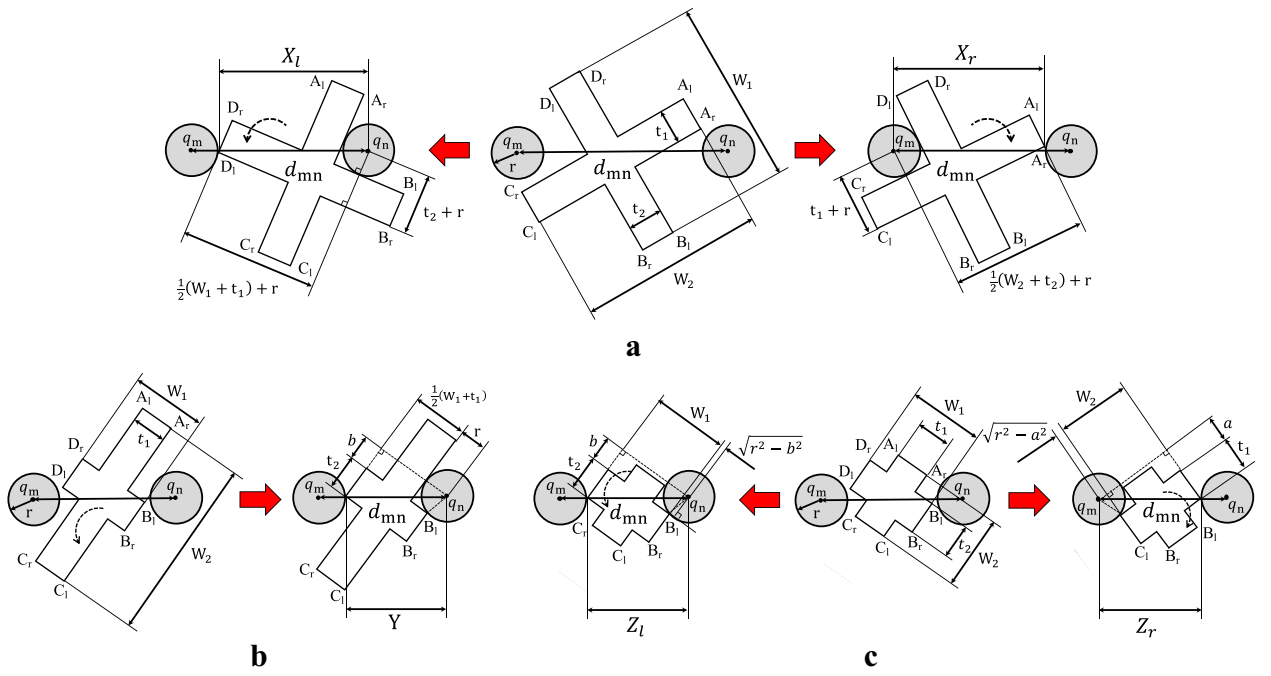


**Fig. 7** Rigid-part caging condition. **a** (i), **b** (ii), and **c** (iii)

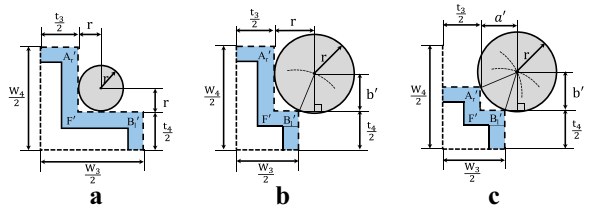


**Fig. 8** Soft-part deformation condition. **a** (i), **b** (ii), and **c** (iv)

### Soft-part deformation condition

This condition indicates that $d_{mn}$ is smaller than the distance at which the finger comes in contact with the concave part of the object soft part without deforming it. Depending on relationships of parameters between the soft part of the object and fingers, the following sufficient conditions are established.

(i) $(W_3 - t_3)/2 \geq r$, and $(W_4 - t_4)/2 \geq r$

In this case, when two sides of the concave part formed in the object soft part ($\overline{A'_r F'}$ and $\overline{B'_l F'}$) are tangent to the finger, this is regarded as the critical state where the object soft part touches the finger (Fig. 8a), and then the soft part is forced to deform when fingers close from this state. As a result, one sufficient condition is expressed as follows:

$$d_{mn} < 2\sqrt{(r + t_3/2)^2 + (r + t_4/2)^2}. \tag{14}$$

(ii) $(W_3 - t_3)/2 < r$, and $(W_4 - t_4)/2 \geq r$

In this case, when one side of the concave part formed in the object soft part ($\overline{A'_r F'}$) is tangent to the finger, and the other side is tangent to the finger at the vertex ($B'_l$), this is regarded as the critical state where the object soft part touches the finger (Fig. 8b). The sufficient condition is expressed as follows:

$$d_{mn} < 2\sqrt{(r + t_3/2)^2 + (b' + t_4/2)^2}, \tag{15}$$

where

$$b' = \sqrt{r^2 - \{r - (W_3 - t_3)/2\}^2}.$$

(iii) $(W_3 - t_3)/2 \geq r$, and $(W_4 - t_4)/2 < r$

In this case, which is opposite condition to (ii), the sufficient condition is as follows:

$$d_{mn} < 2\sqrt{(a' + t_3/2)^2 + (r + t_4/2)^2}, \tag{16}$$

where:

$$a' = \sqrt{r^2 - \{r - (W_4 - t_4)/2\}^2}.$$

(iv) $(W_3 - t_3)/2 < r$, and $(W_4 - t_4)/2 < r$

In this case, when two sides of the concave part formed in the object soft part are tangent to the finger at vertexes ($A'_r$ and $B'_l$), this is regarded as the critical state where the object soft part touches the finger (Fig. 8c). The sufficient condition is expressed as follows:

$$d_{mn} < 2\sqrt{(a' + t_3/2)^2 + (b' + t_4/2)^2}, \tag{17}$$

where

$$\begin{cases} a' = \frac{1}{2}\left(h + \sqrt{\frac{4k^2r^2}{h^2+k^2} - k^2}\right), \\ b' = \frac{1}{2}\left(k + \sqrt{\frac{4h^2r^2}{h^2+k^2} - h^2}\right), \\ k = (W_4 - t_4)/2, \\ h = (W_3 - t_3)/2. \end{cases}$$

### Experimental verification

An experiment was conducted to verify caging-based grasping of the cross-shaped object (Fig. 9a). We used the DENSO WAVE 6-axis manipulator VP-6242G as a robotic arm (Fig. 9b), and the TAIYO 1DOF open/close hand with two circle-shaped fingers as the robotic hand (Fig. 9c). Parameters of the finger and cross-shaped object are defined in Fig. 6, and measurements of the hand and object which were used in this experiment are as follows:

- Hand measurement [mm]: $r = 7$.
- Object measurements [mm]: $W_1 = 79.2$, $W_2 = 79.2$, $W_3 = 99.7$, $W_4 = 100.4$, $t_1 = 15.8$, $t_2 = 15.8$, $t_3 = 35.6$, $t_4 = 38.2$.

This object corresponded to the closed region formation condition (i), and the $d_{mn}$, grasping distance, needed to satisfy the following inequalities:

$$\begin{cases} d_{mn} < \min\{W_1, W_2\} + 2r = 93.2\ [\text{mm}], \\ d_{mn} < \min\{X_l, X_r\} + r = 66.1\ [\text{mm}], \end{cases} \tag{18}$$

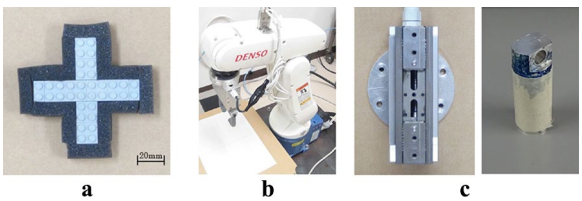


**Fig. 9** Experimental equipment. **a** Manipulator, **b** two-fingered hand, and **c** object

where

$$\begin{cases} X_l = \sqrt{\{(W_1 + t_1)/2 + r\}^2 + (t_2 + r)^2} \\ \quad = 59.1\ [\text{mm}], \\ X_r = \sqrt{\{(W_2 + t_2)/2 + r\}^2 + (t_1 + r)^2} \\ \quad = 59.1\ [\text{mm}]. \end{cases} \tag{19}$$

Next, it was impossible for $d_{mn}$ to become smaller than $d_{mn}$ when the finger touched the concave part of the object rigid part, so the following inequality should be satisfied:

$$d_{mn} \geq 2\sqrt{(r + t_1/2)^2 + (r + t_2/2)^2} = 42.1\ [\text{mm}]. \tag{20}$$

From the above, the distance between the two fingers, $d_{mn}$, had to stay within the following range for satisfying the rigid-part caging condition:

$$42.1\ [\text{mm}] \leq \text{d}_{\text{mn}} < 66.1\ [\text{mm}]. \tag{21}$$

Regarding the soft-part deformation condition, this object corresponded to case (i), and the $d_{mn}$, grasping distance, needed to satisfy the following inequality:

$$d_{mn} < 2\sqrt{(r + t_3/2)^2 + (r + t_4/2)^2} = 72.0\ [\text{mm}]. \tag{22}$$

Through the pick-and-place experiment within the above $d_{mn}$, we set $d_{mn} = 65.0$ [mm] and confirmed the object was grasped by the deformation of the object soft part, as shown in Fig. 10. We also confirmed that the object was caged robustly by disturbing it manually.

## Closed-loop structure

In this section, we introduce a class of caging-based grasping of the closed-loop structure. Concretely, we set targets of caging-based grasping as four-, five-, and six-bar closed-loop structures, and an infinite-bar closed-loop structure (strap). In this paper, we representatively introduce concrete conditions of the four-bar closed-loop structure with a two-fingered hand with the soft part, for 2D caging-based grasping.

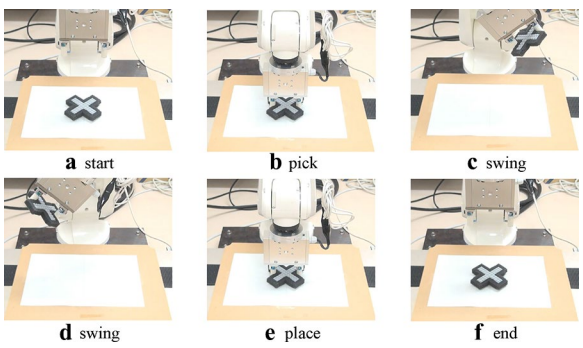


**Fig. 10** Experimental results

### Hand and object model

The hand we use is a two-fingered rigid hand with a soft part. This hand has two circle-shaped 1DOF open/close fingers. The distances between the center of the hand and the fingers ($r_d$) are the same. Also, the soft part surrounds the rigid part, forming a circular shape as shown in Fig. 11a. The four-bar closed-loop structure is shown in Fig. 11b. Parameters of the hand and object are shown as follows:

- $\text{J}_\text{i}$: joint centers ($i = 1 - 4$).
- $q_j$: finger centers ($j = \text{m, n}$).
- $r_{\text{rigid}}$: radius of the rigid part.
- $r_{\text{soft}}$: radius of the soft part.
- $b$: distance between the center of the hand and that of the finger.
- $d_{mn}$: finger center distance.
- $a$: link length.
- $2t$: link thickness.
- $\alpha$: angle between x-axis and link.
- $x', y'$: intersection of perpendicular line dropped from $q_n$ to $\overline{\text{J}_1\text{J}_2}$.

### Rigid-part caging condition

#### *Closed region formation*

In this paper, it is obvious that this condition is satisfied automatically by the existence of the rigid part of the finger, and the closed loop of the object.

### Soft-part deformation condition

This condition indicates that the finger is opened in the range of the $d_{mn}(=2\text{b})$ in a state where the soft part of the finger is inevitable to deform. This range can be calculated from two critical states, in which the rigid/soft parts of the hand are tangent to the link, respectively. Here, the

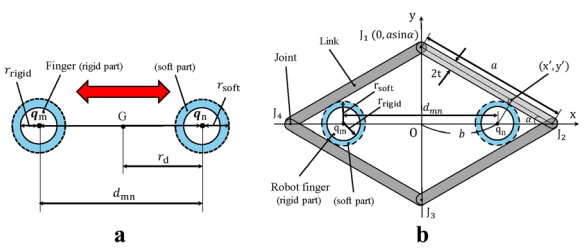


**Fig. 11** Closed-loop structure. **a** Hand and **b** object model

two critical states have to be calculated, because the link structure is deformed by the external force received from the fingers. We call these two states the soft part critical state, in which the loop structure is stretched to the maximum without the deformation of the soft parts, and the rigid part critical state, in which the rigid parts are tangent to the inner part of the link. In other words, when $d_{mn}$ is opened between $2b_{\text{soft\_critical}}$ and $2b_{\text{rigid\_critical}}$, the finger soft part is deformed, which satisfies the soft-part deformation condition:

$$2b_{\text{soft\_critical}} < d_{mn} \leq 2b_{\text{rigid\_critical}}. \tag{23}$$

Also, $b_{\text{soft\_critical}}$ and $b_{\text{rigid\_critical}}$ are expressed as follows:

$$\begin{cases} b_{\text{soft\_critical}} = aY - r/X \text{ when } \mathrm{r} = \mathrm{r}_{\text{soft}}, \\ b_{\text{rigid\_critical}} = aY - r/X \text{ when } \mathrm{r} = \mathrm{r}_{\text{rigid}}. \end{cases} \tag{24}$$

where

$$\begin{cases} X = \dfrac{M^{1/2}L^{1/3}}{12^{1/3}M - 12^{2/3}L^{2/3}}Y, \\ Y = \sqrt{(M + 12^{1/3}L^{2/3} + 6a\,L^{1/3})/6aL^{1/3}}, \\ L = (r+t)^2\left(\sqrt{3}\sqrt{27a^2 + 4r^2 + 8rt + 4t^2} - 9a\right), \\ M = 12^{2/3}(r+t)^2. \end{cases}$$

The derivation of Eq. (24) can be found in Appendix A.

### Experimental verification

An experiment was conducted to verify caging-based grasping of the four-bar closed-loop structure. We used the same robotic arm and hand which was used in the previous section. However, the hand used in this section has soft parts (urethane foam), surrounding the rigid parts, as shown in Fig. 12. Parameters of the finger and four-bar closed-loop structure are defined in Fig. 11, and the measurements of the hand and the object which were used in this experiment are as follows:

- Hand measurements [mm]: $r_{\text{rigid}} = 7, r_{\text{soft}} = 10.5$.
- Object measurements [mm]: $a = 79.9, t = 3.7$.

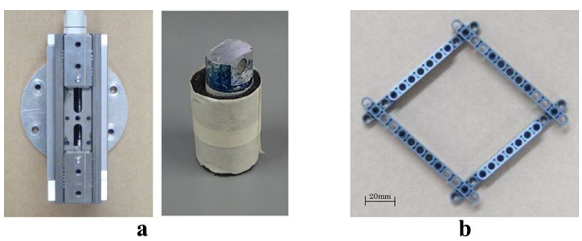

**Fig. 12** Experimental equipment. **a** Two-fingered hand and **b** object model

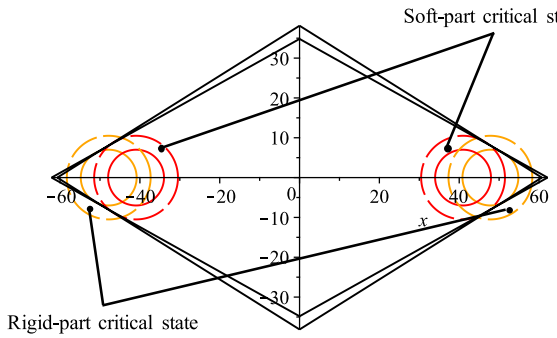


**Fig. 13** Critical states of the soft-part deformation condition

By the above parameters and Eq. (24), the distance between two fingers, $d_{mn}$, had to stay within the following range for satisfying the soft-part deformation condition. Soft- and rigid-part critical states were shown in Fig. 13, which shows only the inner side of the link considering the thickness.

$$81.9\ [\text{mm}] < \mathrm{d}_{\text{mn}} \leq 95.6\ [\text{mm}]. \tag{25}$$

Through the pick-and-place experiment within the above $d_{mn}$, we set $d_{mn} = 88.8$ [mm] and confirmed the object was grasped by the deformation of the hand soft part, as shown in Fig. 14. We also confirmed that the object was caged robustly by disturbing it manually.

## Two rigid bodies connected with a string

In this section, we introduce a class of caging-based grasping of two rigid bodies connected with a string. Concretely, we set the targets of caging-based grasping as two spheres, cuboids, and cylinders connected with a string. In this paper, we representatively introduce concrete conditions of the two cuboids connected with a string with the parallel gripper, which consists of rigid parts and soft parts, for 3D caging-based grasping.

### Hand and object model

The hand we use is a rigid hand with a parallel gripper with soft parts as shown in Fig. 15a. The two cuboids connected with a string are shown in Fig. 15b. Note that the relation of $a$, $b$, $c$ is $a \leq b \leq c$. Not limited to what is shown in Fig. 15b, the positions of $a$, $b$, $c$ can be replaced with each other. The string is non-stretchable and its cross section is circular. The parallel gripper consists of F-shaped rigid fingers with circular cross sections, and soft parts attached to the inner side of the rigid parts. Parameters of the hand and object are shown as follows:

- $r_{\text{rigid}}$: rigid link part radius.
- $r_{\text{string}}$: string radius.
- $T$: jaw tip length.

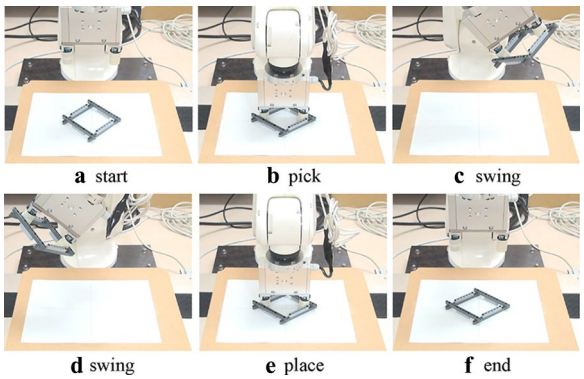


**Fig. 14** Experimental results

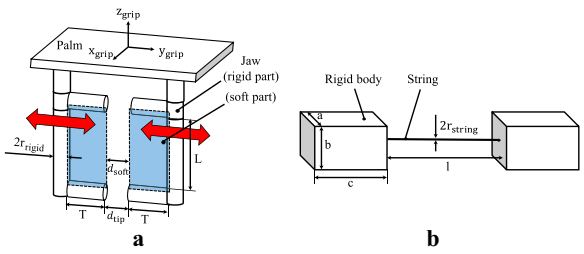


**Fig. 15** Two rigid bodies connected with a string. **a** Hand and **b** object model

- $L$: jaw side length.
- $d_{\text{tip}}$: jaw tip distance.
- $d_{\text{soft}}$: soft part distance in open/close direction of jaw.

## Rigid-part caging condition

### *Closed region formation*

One sufficient condition is preventing the rectangular cross section from passing through the jaws, as well as closing the distance between the jaw tips $d_{\text{tip}}$, so that the string cannot escape from the jaw tips. Firstly, the condition for which the string cannot escape from the jaw tips is as follows:

$$d_{\text{tip}} < 2r_{\text{string}}. \tag{26}$$

In order to prevent the rectangular cross section from escaping in the longitudinal (Fig. 16a) and lateral (Fig. 16b) direction, respectively, the following conditions have to be satisfied:

$$2T + d_{\text{tip}} < a \quad \text{or} \quad \text{L} < \text{b}, \tag{27}$$

$$2T + d_{\text{tip}} < b \quad \text{or} \quad \text{L} < \text{a}. \tag{28}$$

In the diagonal direction (Fig. 16c), two simultaneous equations which form the critical state (Fig. 16e), can be drawn as below:

$$\alpha = \sin^{-1}\frac{L}{\sqrt{a^2+b^2}} - \tan^{-1}\frac{a}{b}, \tag{29}$$

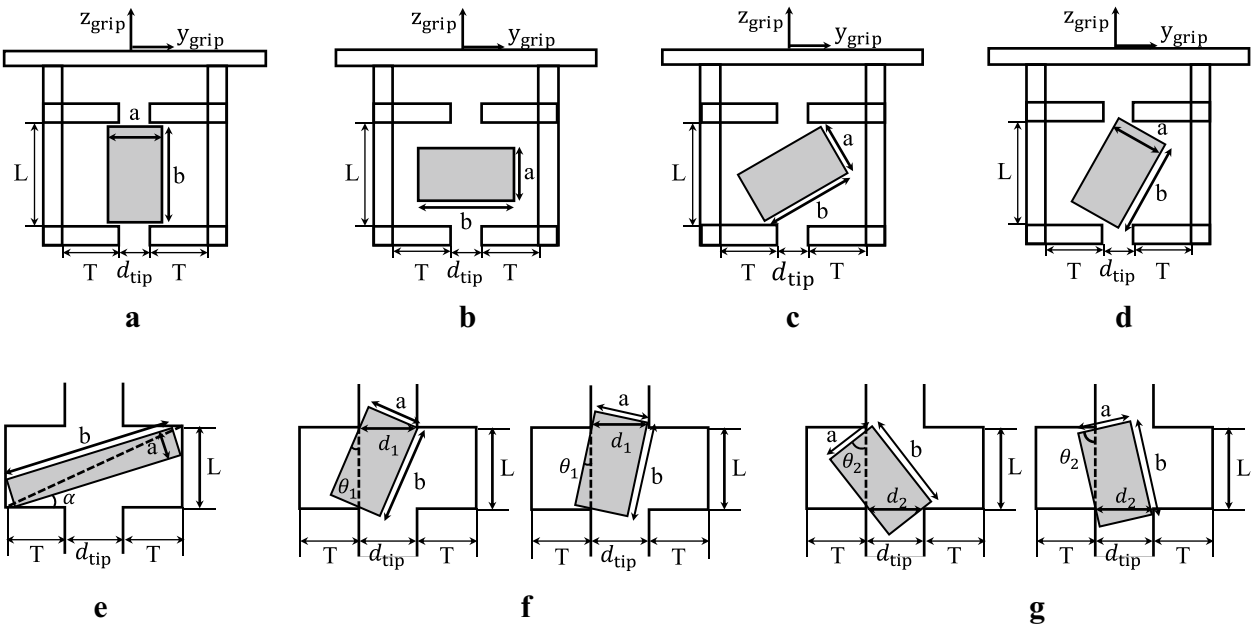


**Fig. 16** Rigid-part caging condition. **a** Longitudinal, **b** lateral, **c** diagonal (i), and **d** diagonal (ii) directions. Also, **e** Critical state of **c**, and **f**, **g** critical states of **d**

$$2T + d_{\text{tip}} = a\sin\alpha + b\cos\alpha. \tag{30}$$

The condition which prevents the object from escaping in the diagonal direction can be expressed from Eq. (30), as below:

$$d_{\text{tip}} < a\sin\alpha + b\cos\alpha - 2T. \tag{31}$$

Thus, in $a\sin\alpha + b\cos\alpha$, $\alpha$ can be eliminated by transforming Eq. (29), which is derived in Appendix B. So Eq. (31) can be converted as below:

$$d_{\text{tip}} < \frac{2abL + (b^2 - a^2)\sqrt{a^2 + b^2 - L^2}}{a^2 + b^2} - 2T. \tag{32}$$

In addition to the above states, the state where part of the rectangular cross section enters into the gap between the jaw tip and the upper part (Fig. 16d) should also be considered. When satisfying $\sqrt{a^2 + b^2} > L$, the critical state is shown as Fig. 16f, and projection of the upper ($d_{11}(\theta_1)$) and lower ($d_{12}(\theta_1)$) parts are respectively expressed as:

$$d_{11}(\theta_1) = \begin{cases} \frac{b - L\cos\theta_1}{\sin\theta_1}, & \left(\frac{b - L\cos\theta_1}{\sin\theta_1} \le \frac{a}{\cos\theta_1}\right) \\ \frac{a}{\cos\theta_1}. & \left(\frac{b - L\cos\theta_1}{\sin\theta_1} > \frac{a}{\cos\theta_1}\right) \end{cases} \tag{33}$$

$$d_{12}(\theta_1) = \frac{a - L\sin\theta_1}{\cos\theta_1}. \tag{34}$$

The larger projection is given by:

$$d_1(\theta_1) = \max\{d_{11}(\theta_1), d_{12}(\theta_1)\}. \begin{cases} 0 \le \theta_1 \le \frac{\pi}{2} & (b > L, a > L) \\ 0 \le \theta_1 \le \sin^{-1}\frac{a}{L} & (b > L, a \le L) \\ \cos^{-1}\frac{b}{L} \le \theta_1 \le \sin^{-1}\frac{a}{L} & (b \le L, a \le L) \end{cases} \tag{35}$$

When replacing the side part of $a$, $b$ as Fig. 16g, there is no need to consider this additionally, because it is the reverse formation of the Fig. 16f. Calculating the minimum $d_1(\theta_1)$ is equivalent to satisfying the critical state, in which the object cannot escape from the gripper. This can be expressed as below:

$$d_{\text{tip}} < \min_{\theta_1} d_1(\theta_1). \tag{36}$$

With the above conditions, in sum, closed region formation can be expressed as below:

$$\begin{cases} 2T + d_{\text{tip}} < a \quad \text{or} \quad \text{L} < \text{b}, \\ 2T + d_{\text{tip}} < b \quad \text{or} \quad \text{L} < \text{a}, \\ d_{\text{tip}} < \frac{2abL + (b^2 - a^2)\sqrt{a^2 + b^2 - L^2}}{a^2 + b^2} - 2T \\ \qquad \text{or} \quad \sqrt{\text{a}^2 + \text{b}^2} \le \text{L}, \\ d_{\text{tip}} < \min_{\theta_1} d_1(\theta_1) \quad \text{or} \quad \sqrt{\text{a}^2 + \text{b}^2} \le \text{L}, \\ d_{\text{tip}} < 2r_{\text{string}}. \end{cases} \tag{37}$$

### Soft-part deformation condition

When the cylinder-shaped string touches the two soft parts of the gripper, this is regarded as the critical state. The soft-part deformation condition is then satisfied when the diameter of the string is longer than the distance between the two soft parts of the gripper $d_{\text{soft}}$ deforming the soft parts (Fig. 17). The sufficient condition is expressed as below:

$$d_{\text{soft}} < 2r_{\text{string}}. \tag{38}$$

### Experimental verification

An experiment was conducted to verify caging-based grasping of the two cuboids connected with a string. We used the same robotic arm and hand which was used in the previous section, except that the jaws were attached as shown in Fig. 18. Parameters of the hand and two cuboids connected with a string are defined in Fig. 15, and measurements of the hand and object, which were used in this experiment, are as follows:

- Hand measurements [mm]: $L = 30.7$, $T = 20.0$, $r_{\text{rigid}} = 7$.
- Object measurements [mm]: $a = 25.1$, $b = 45.1$, $c = 55.2$, $r_{\text{string}} = 2.5$, $l = 100$.

By Eq. (37), the closed region condition was satisfied when $d_{\text{tip}}$ was as below:

$$d_{\text{tip}} < 5.0\ [\text{mm}]. \tag{39}$$

Also, the soft part of the parallel gripper which we used had the relation, $d_{\text{soft}} = d_{\text{tip}} - 4.8$ [mm], so considering Eq. (38), the soft-part deformation condition was satisfied when $d_{\text{tip}}$ was as below:

$$d_{\text{tip}} < 9.8\ [\text{mm}]. \tag{40}$$

Through conducting pick-and-place within the above $d_{mn}$, we set $d_{mn} = 4.0$ [mm] and confirmed the object was grasped by deformation of the gripper soft part as shown in Fig. 19. We also confirmed that the object was caged robustly by disturbing it manually.

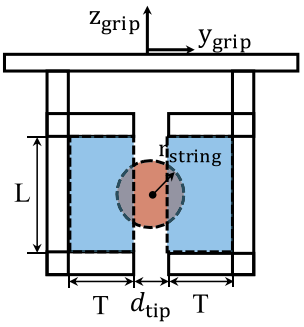


**Fig. 17** Soft-part deformation condition

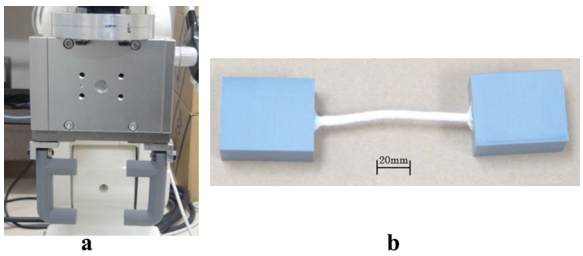


**Fig. 18** Experimental equipment. **a** Parallel gripper and **b** object model

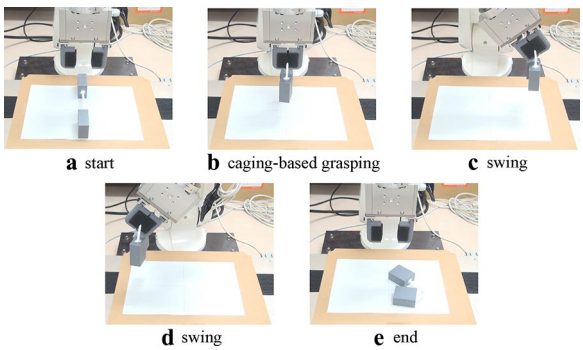


**Fig. 19** Experimental results

## Discussion and conclusion

In this study, we proposed a method of caging-based grasping to manipulate deformable objects with only geometric constraints. We firstly formulated the caging-based grasping approach of deformable objects. This was realized by caging of the objects by rigid parts of hands with deformations of soft parts. This formulation was defined using only shape information, which consists of rigid-part caging condition and a soft-part deformation condition, even for deformable objects. Next, three types of deformable objects: a rigid object covered with a soft part, a closed-loop structure, and two rigid bodies connected with a string are defined as deformable objects. These can be regarded as the primitive shapes of deformable objects. In these types, soft parts, joints, and strings were regarded as the deformable components, respectively. Also, we derived concrete conditions for grasp synthesis as sufficient conditions respectively. Through pick-and-place experiments, we confirmed that it was possible to manipulate deformable objects with caging-based grasping, simply by knowing the shape information of the objects.

There are also limitations of our proposed method as a tradeoff. When closing the robotic hands for satisfying the caging-based grasping condition, we set $d_{mn}$ (or $d_{\mathrm{tip}}$) properly in the range of calculated results. However, object weights or insufficient friction causes objects to slide and escape from the hands in the case of 2D caging-based grasping. For solving this problem, calculating the optimized $d_{mn}$, which maximizes the margin spaces of closed regions, also remains as future works.



**Authors' contributions**
YM proposed the basic formulation of the proposed method, checked the manuscript, and carried out the conceptual supervising. DK revised the formulation of the proposed method, derived the concrete conditions, designed and carried out the experiments, analyzed the experimental results, and wrote the manuscript. SK checked the derived conditions, and corrected errors found in them. All authors read and approved the final manuscript.

**Author details**
[1] Department of Precision Engineering, The University of Tokyo, 7-3-1 Hongo, Bunkyo-ku, 113-8656 Tokyo, Japan. [2] Faculty of Engineering, Yokohama National University, 79-5 Tokiwadai, Hodogaya-ku, 240-8501 Yokohama, Japan. [3] Department of Mechanical Engineering and Materials Science, Yokohama National University, 79-5 Tokiwadai, Hodogaya-ku, 240-8501 Yokohama, Japan.

**Acknowledgements**
Not applicable.

**Competing interests**
The authors declare that they have no competing interests.

**Availability of data and materials**
The data that support the findings of this study are available from the corresponding author upon reasonable request.

**Funding**
This work was supported by Yokohama National University.

## Appendix A: derivation of Eq. (24)

To calculate the $b_{\mathrm{soft\_critical}}$ and $b_{\mathrm{rigid\_critical}}$, the following conditions have to be satisfied:

- $(x', y')$ exists on the straight line which is expressed as $y = -\tan\alpha \cdot x + a\sin\alpha$.
- The distance from $q_{\mathrm{n}}$ to $(x', y')$ is equal to $r + t$.

Considering above conditions, the following equations are derived:

$$\frac{y'}{\sin\alpha} + \frac{x'}{\cos\alpha} = a\sin\alpha, \tag{41}$$

$$x' = b + (r+t)\sin\alpha, \tag{42}$$

$$y' = (r+t)\cos\alpha. \tag{43}$$

When summarized in the expression relating to $b$:

$$b = a\cos\alpha - \frac{r+t}{\sin\alpha}. \tag{44}$$

In order to derive the $\alpha$ which maximizes $b$, the partial differential of $b$ with respect to $\alpha$ is calculated, and the $\alpha$ which makes it equal to zero shows the critical states:

$$\frac{\partial b}{\partial \alpha} = -a\sin\alpha + \frac{(r+t)\cos\alpha}{\sin^2\alpha} = 0, \tag{45}$$

which can be expressed as below:

$$\frac{\sin^3\alpha}{\cos\alpha} = \frac{r+t}{a}. \tag{46}$$

When considering the above equations and the Pythagorean trigonometric identity, two non-linear simultaneous equations can be derived as below:

$$\frac{X^3}{Y} = \frac{r+t}{a}, \tag{47}$$

$$X^2 + Y^2 = 1, \tag{48}$$

where

$$X = \sin\alpha,\ Y = \cos\alpha.$$

By solving the above equations, $X$ and $Y$ are obtained, and $b$ is eventually calculated as below:

$$\begin{cases} b_{\text{soft\_critical}} = aY - r/X & \text{when } \mathrm{r} = \mathrm{r}_{\text{soft}}, \\ b_{\text{rigid\_critical}} = aY - r/X & \text{when } \mathrm{r} = \mathrm{r}_{\text{rigid}}. \end{cases} \tag{49}$$

where

$$\begin{cases} X = \dfrac{M^{1/2}L^{1/3}}{12^{1/3}M - 12^{2/3}L^{2/3}}Y, \\ Y = \sqrt{(M + 12^{1/3}L^{2/3} + 6aL^{1/3})/6aL^{1/3}}, \\ L = (r+t)^2\left(\sqrt{3}\sqrt{27a^2 + 4r^2 + 8rt + 4t^2} - 9a\right), \\ M = 12^{2/3}(r+t)^2. \end{cases}$$

In Eq. (49), $r$ can be replaced with $r_{\text{rigid}}$ or $r_{\text{soft}}$ for considering rigid part and soft part critical states, respectively.

## Appendix B: derivation of Eq. (32)

When given Eq. (50) as below:

$$\alpha = \sin^{-1}\frac{L}{\sqrt{a^2+b^2}} - \tan^{-1}\frac{a}{b}. \tag{50}$$

$\sin\alpha$ and $\cos\alpha$ are calculated using trigonometric addition formulas, and are expressed as follows:

$$\begin{aligned} \sin\alpha &= \sin\left(\sin^{-1}\frac{L}{\sqrt{a^2+b^2}} - \tan^{-1}\frac{a}{b}\right) \\ &= \sin\left(\sin^{-1}\frac{L}{\sqrt{a^2+b^2}}\right)\cos\left(\tan^{-1}\frac{a}{b}\right) \\ &\quad - \cos\left(\sin^{-1}\frac{L}{\sqrt{a^2+b^2}}\right)\sin\left(\tan^{-1}\frac{a}{b}\right) \\ &= \frac{L}{\sqrt{a^2+b^2}}\cdot\frac{b}{\sqrt{a^2+b^2}} \\ &\quad - \frac{\sqrt{a^2+b^2-L^2}}{\sqrt{a^2+b^2}}\cdot\frac{a}{\sqrt{a^2+b^2}} \\ &= \frac{bL - a\sqrt{a^2+b^2-L^2}}{a^2+b^2}. \end{aligned} \tag{51}$$

$$\begin{aligned} \cos\alpha &= \cos\left(\sin^{-1}\frac{L}{\sqrt{a^2+b^2}} - \tan^{-1}\frac{a}{b}\right) \\ &= \cos\left(\sin^{-1}\frac{L}{\sqrt{a^2+b^2}}\right)\cos\left(\tan^{-1}\frac{a}{b}\right) \\ &\quad + \sin\left(\sin^{-1}\frac{L}{\sqrt{a^2+b^2}}\right)\sin\left(\tan^{-1}\frac{a}{b}\right) \\ &= \frac{L}{\sqrt{a^2+b^2}}\cdot\frac{a}{\sqrt{a^2+b^2}} \\ &\quad + \frac{\sqrt{a^2+b^2-L^2}}{\sqrt{a^2+b^2}}\cdot\frac{b}{\sqrt{a^2+b^2}} \\ &= \frac{aL + b\sqrt{a^2+b^2-L^2}}{a^2+b^2}. \end{aligned} \tag{52}$$

To summarize the above Eqs. (51) and (52), $a\sin\alpha + b\cos\alpha$ is expressed as follows:

$$a\sin\alpha + b\cos\alpha = \frac{2abL + (b^2-a^2)\sqrt{a^2+b^2-L^2}}{a^2+b^2}. \tag{53}$$

Finally, the $d_{\text{tip}}$ which prevents the object from escaping in the diagonal direction is expressed as follows:

$$d_{\text{tip}} < \frac{2abL + (b^2-a^2)\sqrt{a^2+b^2-L^2}}{a^2+b^2} - 2T. \tag{54}$$

Received: 31 December 2018 Accepted: 18 March 2019
Published online: 27 March 2019

**References**

1. Prattichizzo D, Malvezzi M, Bicchi A (2010) On motion and force controllability of grasping hands with postural synergies. In: Proceedings of robotics: science and systems. Zaragoza, Spain, pp 49–56
2. Righetti L, Kalakrishnan M, Pastor P, Binney J, Kelly J, Voorhies RC et al (2014) An autonomous manipulation system based on force control and optimization. Auton Robots 36(1):11–30
3. Rimon E, Blake A (1999) Caging planar bodies by one-parameter two-fingered gripping systems. Int J Rob Res 18(3):299–318
4. Makita S, Wan W (2017) A survey of robotic caging and its applications. Adv Robot 31(19–20):1071–1085
5. Wang Z, Hirata Y, Kosuge K (2005) An algorithm for testing object caging condition by multiple mobile robots. In: 2005 IEEE/RSJ international conference on intelligent robots and systems, pp 3022–3027
6. Wan W, Shi B, Wang Z, Fukui R (2017) Multirobot object transport via robust caging. In: IEEE transactions on systems, man, and cybernetics: systems, pp 1–11
7. Kwok T, Wan W, Pan J, Wang CCL, Yuan J, Harada K, et al. (2016) Rope caging and grasping. In: 2016 IEEE international conference on robotics and automation, pp 1980–1986
8. Liu J, Xin S, Gaol Z, Xu K, Tu C, Chen B (2018) Caging loops in shape embedding space: theory and computation. In: 2018 IEEE international conference on robotics and automation, pp 1–5
9. Maeda Y, Kodera N, Egawa T (2012) Caging-based grasping by a robot hand with rigid and soft parts. In: 2012 IEEE international conference on robotics and automation, pp 5150–5155
10. Egawa T, Maeda Y, Tsuruga H (2015) Two- and three-dimensional caging-based grasping of objects of various shapes with circular robots and multi-fingered hands. In: IECON 2015—41st annual conference of the IEEE industrial electronics society, pp 000643–000648
11. Vahedi M, van der Stappen AF (2008) Caging polygons with two and three fingers. Int J Rob Res 27(11–12):1308–1324
12. Lei Q, Wisse M (2016) Object grasping by combining caging and force closure. In: 2016 14th international conference on control, automation, robotics and vision, pp 1–8
13. Pipattanasomporn P, Makapunyo T, Sudsang A (2016) Multifinger caging using dispersion constraints. IEEE Trans Robot 32(4):1033–1041
14. Bunis HA, Rimon ED, Golan Y, Shapiro A (2017) Caging polygonal objects using equilateral three-finger hands. IEEE Robot Autom Lett 2(3):1672–1679
15. Gopalakrishnan KG, Goldberg K (2005) D-space and deform closure grasps of deformable parts. Int J Rob Res 24(11):899–910
16. Varava A, Kragic D, Pokorny FT (2016) Caging grasps of rigid and partially deformable 3-D objects with double fork and neck features. IEEE Trans Robot 32(6):1479–1497
17. Jia Y, Guo F, Tian J (2011) On two-finger grasping of deformable planar objects. In: 2011 IEEE international conference on robotics and automation, pp 5261–5266
18. Lin H, Guo F, Wang F, Jia YB (2015) Picking up a soft 3D object by "feeling" the grip. Int J Rob Res 34(11):1361–1384
19. Hirai S, Tsuboi T, Wada T (2001) Robust grasping manipulation of deformable objects. In: Proceedings of the 2001 IEEE international symposium on assembly and task planning, pp 411–416
20. Khalil FF, Curtis P, Payeur P (2010) Visual monitoring of surface deformations on objects manipulated with a robotic hand. In: 2010 IEEE international workshop on robotic and sensors environments, pp 1–6
21. Su J, Qiao H, Ou Z, Liu ZY (2015) Vision-based caging grasps of polyhedron-like workpieces with a binary industrial gripper. IEEE Trans Autom Sci Eng 07(12):1–14